Image volume analysis of omnidirectional parallax regular-polyhedron three-dimensional displays

Hwi Kim, Joonku Hahn, and Byoungho Lee*

School of Electrical Engineering, Seoul National University
Gwanak-Gu Gwanakro 599, Seoul 151-744, Korea
**Corresponding author: byoungho@snu.ac.kr*
http://oeqelab.snu.ac.kr

Abstract: Three-dimensional (3D) displays having regular-polyhedron structures are proposed and their imaging characteristics are analyzed. Four types of conceptual regular-polyhedron 3D displays, i.e., hexahedron, octahedron, dodecahedron, and icosahedrons, are considered. In principle, regular-polyhedron 3D display can present omnidirectional full parallax 3D images. Design conditions of structural factors such as viewing angle of facet panel and observation distance for 3D display with omnidirectional full parallax are studied. As a main issue, image volumes containing virtual 3D objects represented by the four types of regular-polyhedron displays are comparatively analyzed.

OCIS codes: (080.0080) Geometric optics, (110.0110) Imaging systems

References and links

1. R. Lopez-Gulliver, S. Yoshida, S. Yano, and N. Inoue, "gCubik: a cubic autostereoscopic display for multiuser interaction – grasp and group-share virtual images," ACM SIGGRAPH 2008, Poster Proceedings, 133, (2008).
2. B. Lee, J.-H. Park, and S.-W. Min, "Three-dimensional display and information processing based on integral imaging," in *Digital Holography and Three-Dimensional Display*, T.-C. Poon, ed. (Springer, 2006), pp. 333-378.
3. R. Lopez-Gulliver, S. Yoshida, S. Yano, and N. Inoue, "Toward an interactive box-shaped 3d display: study of the requirements for wide field of view," IEEE Symposium on 3D User Interfaces, 157-158 (2008).
4. I. Stavness, F. Vogt, and S Fels, "Cubee: A Cubic 3D display for physics-based interaction," ACM SIGGRAPH 2006, Sketches, 165 (2006).
5. A. Jones, I. McDowall, H. Yamada, M. Bolas, and P. Debevec, "An interactive 360° light field display," ACM SIGGRAPH 2007, Emerging Technologies, 13 (2007).
6. Y. Kim, J.-H. Park, H. Choi, S. Jung, S.-W. Min, and B. Lee, "Viewing-angle-enhanced integral imaging system using a curved lens array," Opt. Express **12**, 421-429 (2004).
7. J. Hahn, H. Kim, Y. Lim, G. Park, and B. Lee, "Wide viewing angle dynamic holographic stereogram with a curved array of spatial light modulators," Opt. Express **16**, 12372-12386 (2008).
8. H. Kim, J. Hahn, and B. Lee, "The use of a negative index planoconcave lens array for wide-viewing angle integral imaging," Opt. Express **16**, 21865-21880 (2008).
9. R. Martinez-Cuenca, H. Navarro, G. Saavedra, B. Javidi, and M. Martinez-Corral, "Enhanced viewing-angle integral imaging by multiple-axis telecentric relay system," Opt. Express **15**, 16255-16260 (2007).
10. S.-H. Shin and B. Javidi, "Viewing-angle enhancement of speckle-reduced volume holographic three-dimensional display by use of integral imaging," Appl. Opt. **41**, 5562-5567 (2002).
11. Y. Takaki, "Thin-type natural three-dimensional display with 72 directional images," Proc. SPIE **5664**, 56-63 (2005).
12. D.-H. Shin, B. Lee, and E.-S. Kim, "Effect of illumination in an integral imaging system with large depth of focus," Appl. Opt. **44**, 7749-7753 (2005).
13. M.-O. Jeong, N. Kim, and J.-H. Park, "Elemental image synthesis for integral imaging using phase-shifting digital holography," J. Opt. Soc. Korea **12**, 275-280 (2008).

#107004 - $15.00 USD Received 30 Jan 2009; revised 24 Mar 2009; accepted 1 Apr 2009; published 2 Apr 2009

14. M.-S. Kim, G. Baasantseren, N. Kim, and J.-H. Park, "Hologram generation of 3D objects using multiple orthographic view images," J. Opt. Soc. Korea **12**, 269-274 (2008).

1. Introduction

Recently an interesting invention of three-dimensional (3D) display, gCubik, attracted much attention in the research and development society of 3D displays [1]. The gCubik is a volumetric autostereoscopic display with regular-hexahedron shape whose facets are flat integral imaging (integral photography; IP) display panels [2, 3]. Each integral imaging panel is especially designed to have 60 (deg.) viewing angle [3]. Thus omnidirectional parallax is attainable with the gCubik in principle. The concept of realizing omnidirectional parallax with flat 3D panels extended the boundary of design of 3D display systems. Besides the gCubik, there are a few interesting works with respect to the omnidirectional parallax. The cubic 3D display concept with head tracking was reported in [4]. Omnidirectional full parallax 3D display with projection technique and rotating mirror system was proposed in [5]. In the flat panel based volumetric autostereoscopic 3D display such as gCubik, flat facet panels having wide viewing angle are necessary. However, the viewing angle of most present flat panel 3D displays is very limited to narrow viewing angle range. Thus, the development of 60 (deg.) viewing angle IP for the gCubik is interesting and important, which is essential for making the gCubik. As for the gCubik, the critical factor of the regular-polyhedron volumetric display is wide-viewing angle facet panel. The viewing angle enhancement is one of the most important topics associated with the flat panel 3D display [6-14]. There have been researches on the use of curved structures for enhancing viewing angle associated with IP [6] and computer-generated hologram (CGH) [7].

The concept of flat panel based volumetric autostereoscopic 3D display initiated by the development of the gCubik can be extended to more general geometrical structures such as regular-polyhedrons, semi-regular-polyhedrons and the extreme case of perfect sphere. In this paper, four types of regular-polyhedron autostereoscopic 3D display, hexahedron, octahedron, dodecahedron, and icosahedron, are proposed. Although the tetrahedron is a regular-polyhedron, the use of the tetrahedron for the polyhedron 3D display is not attractive since the dihedral angle between two adjacent facets is too large. Thus, four types of regular-polyhedron 3D display are mainly considered. The structural conditions that regular-polyhedron displays become omnidirectional autostereoscopic 3D displays are investigated. An important evaluation factor for omnidirectional volumetric 3D display is the size of image volume. 3D object contents are placed inside the regular-polyhedron shell structure of the regular-polyhedron 3D display. The maximum size of common volume that can be omnidirectionally represented by the display is defined as the image volume size. The functional relationships of the image volume size to structural factors of 3D displays such as facet panel viewing angle and observation distance are analyzed with numerical analysis.

In Section 2, the concept and imaging properties of regular-polyhedron 3D displays are described. The limitation of the representation of 3D object caused by finite viewing angle of facet 3D panels is accounted for. In Section 3, the analysis of the image volume size for four types of regular polyhedron 3D display is presented. The size of the image volume is analyzed with particular focus on the relationship between the facet display viewing angle and the observer's distance. In Section 4, concluding remarks and perspective of polyhedron 3D display are given.

2. Imaging properties of regular-polyhedron three-dimensional displays

In this Section, the basic structures of regular-polyhedron 3D displays and their imaging properties are addressed. Figures 1(a), 1(b), 1(c), and 1(d) show conceptual structures of four types of regular-polyhedron volumetric 3D displays; hexahedron, octahedron, dodecahedron, and icosahedron, respectively. Regular-polyhedron displays are composed of several facets

#107004 - $15.00 USD Received 30 Jan 2009; revised 24 Mar 2009; accepted 1 Apr 2009; published 2 Apr 2009

which are assumed to be ideal 3D flat panel display with a finite viewing angle of θ. In Figs. 1(a)-1(d), an example 3D object is shown together inside each regular-polyhedron.

In principle, one can see omnidirectional virtual views of the 3D object through the facet panels of the regular-polyhedron 3D displays. In practice, IP or CGH panels can be used as facet display of polyhedron display. However, in this paper the practical use of various 3D flat panels is not detailed. We focus on theoretical issues related to the regular-polyhedron structures. The major critical structural factor putting a limitation in representing 3D images is the finite viewing angle of facet panel.

Only a part of the whole surfaces of polyhedrons can actually contribute to displaying to observer, which is structurally determined by viewing angle and observation distance. Specific light rays whose radiation angles measured from the normal vector to the ray direction are less than viewing angle θ contribute to form projection image of the 3D object for observer located at a specific position. Therefore some parts of the 3D object cannot be seen to observer when the facet viewing angle is not large enough. For regular-polyhedron structures, the volume portion of the 3D object that is seen varies according to spatial position of observer because regular-polyhedron structures have finite facets and finite symmetry.

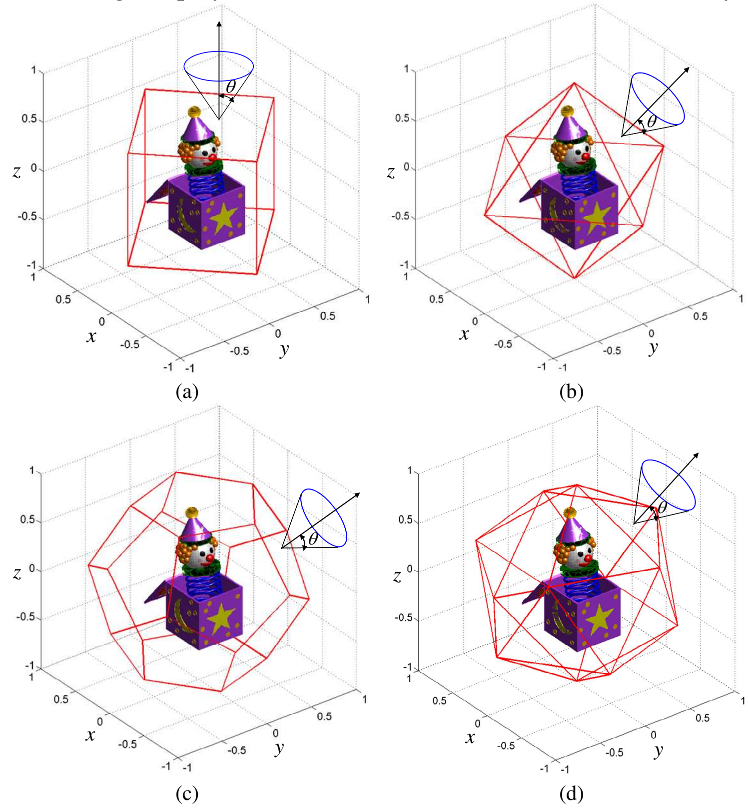

Fig. 1. Four regular-polyhedron displays: (a) hexahedron, (b) octahedron, (c) dodecahedron, and (d) icosahedron.

In Fig. 2, the effect of viewing angle limitation stated above is illustrated for all regular-polyhedron displays. In up and down pictures of right-hand side of Fig. 2(a), projection images of the target 3D object observed at two different positions of the same observation distance, $R = 2$, and directions of (A) $(0.707, -0.707, 0)$ and (B) $(-0.8165, 0, 0.5774)$ through regular-hexahedron display with facet viewing angle of 60(deg.) are shown. All regular-polyhedrons in Fig. 2 are inscribed in a unit sphere with radius of 1. For each direction (A) and (B), due to the limitation of the viewing angle of the facet display, the area on the

#107004 - $15.00 USD Received 30 Jan 2009; revised 24 Mar 2009; accepted 1 Apr 2009; published 2 Apr 2009

surface of the polyhedron through which rays can transfer image information to observer is limitedly localized, which is indicated by cross-marks colored by blue and red, respectively. The obtained set of spatial points on the polyhedron surface is referred to observation window, which is obtained by numerical algorithm. When the angle between outward normal vector at a point and vector from the point to the observation is less than the facet viewing angle θ, the point is included to the observation window. Then an observer can actually see the portion of the projected image that is overlapped with the projection image of the observation window. In the right-hand side images of each figure in Fig. 2, the projection of observable area to the observer is indicated by overlapping. In the case of hexagonal display, at the position (A), whole of the projected image is observable, while at the position (B), the region indicated by the red cross-marks in the projection image of the 3D object is the observable portion. By the same manner, in Figs. 2(b), 2(c), and 2(d), observable projected images for two observation points through octahedron, dodecahedron, and icosahedron displays are presented. In Figs. 2(a) and 2(b), the viewing angle of the facet displays is set to $60(\deg.)$. In Figs. 2(c) and 2(d), the viewing angle of the facet displays is set to $45(\deg.)$.

For a projection image, an inner circle can be defined as a maximum radius, R_i, of internal circle enclosed by the projection image of the observation window. In the right-side images of Figs. 2(a)-2(d), the black circles are indicated in this way. Then R_i is a function, $R_i(\theta, R, \mathbf{d})$, of facet viewing angle θ and observation position (distance R and direction $\mathbf{d}$). The maximum internal circle of the observation window is calculated by numerical algorithm that finds the closed polygon enclosing the sampled cross-marks indicating the observable window area and, after that, obtains the maximum internal circle radius bordering on the inside of the closed polygon.

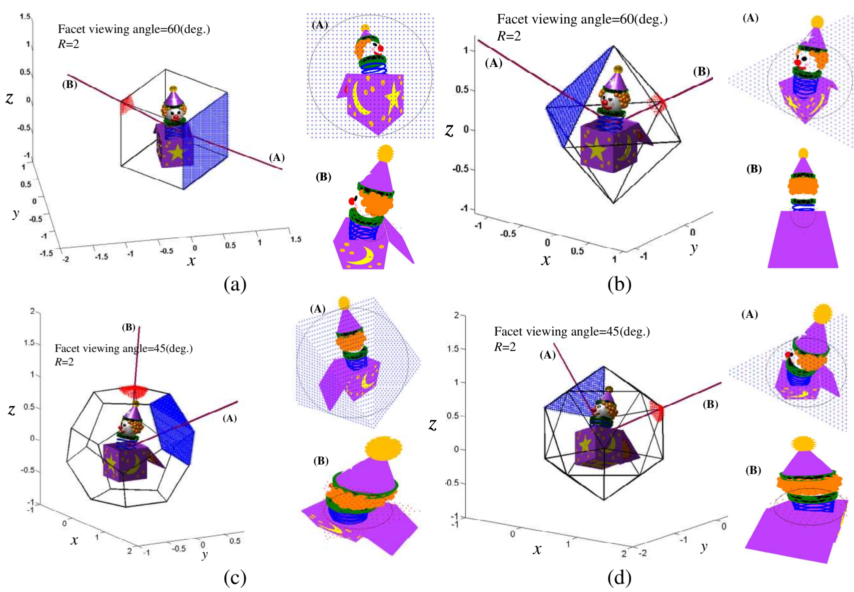

Fig. 2. Observation windows of (a) hexahedron, (b) octahedron, (c) dodecahedron, and (d) icosahedron displays, and observable images through them. Facet viewing angles for (a), (b), (c) and (d) are set to $60(\deg.)$, $60(\deg.)$, $45(\deg.)$, and $45(\deg.)$, respectively.

3. Image volume analysis of regular polyhedron displays

In this Section, the image volume of regular-polyhedron display is defined and respective image volumes of four regular-polyhedron 3D displays are analyzed and compared. Regular-polyhedron is composed of the same kind of regular-polygon facets. Regular-rectangle and

#107004 - $15.00 USD Received 30 Jan 2009; revised 24 Mar 2009; accepted 1 Apr 2009; published 2 Apr 2009

regular-pentagon are composition facets of hexahedron and dodecahedron, respectively. Regular triangle is the composition facet of octahedron and icosahedron.

Inside the regular polyhedron, a common volume exists, which is a spatial volume that can be observed by any observer located on every point on the sphere with a radius of R. From the symmetry of regular-polyhedrons, we can imply that the image volume of the regular-polyhedron has the same symmetry with the corresponding regular-polyhedron. For hexahedron, the image volume has six-axis symmetry since the number of facets of the hexahedron is six. For icosahedron, the image volume has the twenty-axis symmetry. The mathematical geometry of the exact image volume is of interest in theoretical point of view. However, exact geometrical analysis of the image volume shape is beyond this paper. In this paper, the inscribed internal sphere of the exact image volume is used as a measure of the image volume size instead of the exact mathematical image volume. Let us refer this to spherical image volume of regular-polyhedron display.

According to the definition, we can see that any 3D object enclosed by the spherical image volume is seen by any observer located on a sphere surface with radius of R. The radius of the spherical image volume is a function of the facet panel viewing angle θ and the observation distance, R. As the facet viewing angle increases, the radius of the spherical image volume also increases. Several imaging properties of polyhedron 3D displays are discussed with numerical analysis. The most important property is the functional relationship of the radius of spherical image volume to the observation distance and the facet viewing angle.

The numerical calculation is performed by repetitive computation of the maximum internal circle radius as shown in Fig. 2. for every observation direction. Then, we can obtain a radius function, $R_i(\theta, R, \mathbf{d})$ that is radius of inscribed circle of projection image of the observation window of a polyhedron display for the observation direction vector, $\mathbf{d}$. Let the minimum radius of $R_i(\theta, R, \mathbf{d})$ be denoted by R'_v,

$$R'_v(\theta, R) = \min R_i(\theta, R, \mathbf{d}) \quad \text{for} \quad \forall \mathbf{d}. \tag{1}$$

Before further discussing the spherical image volume of the regular-polyhedron, let us examine the image volume of a sphere display. Although we deal with the regular-polyhedron types, the analysis of the sphere type display is necessary for understanding the limitation of the image volume of the regular polyhedron display. Sphere can be seen as a special semi-regular polyhedron with infinite number of facets.

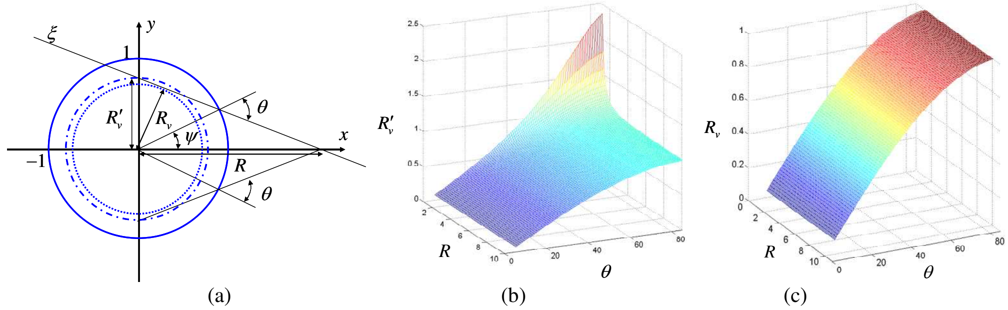

Fig. 3. (a) Observation geometry of spherical display, (b) R'_v and (c) R_v as a function of observation distance R and facet viewing angle θ.

In Fig. 3(a), an observer located on a position $(R,0,0)$ sees a unit sphere display. The point viewing angle of the sphere display is set to θ. Then the observer can see the cross-section of circular cone with apex angle ψ and the sphere as shown in Fig. 3(a). The apex angle of the circular cone is given by, from the geometry of Fig. 3(a),

#107004 - $15.00 USD Received 30 Jan 2009; revised 24 Mar 2009; accepted 1 Apr 2009; published 2 Apr 2009

$$\cos\psi = \frac{\sin^2\theta + \cos\theta\sqrt{R^2 - \sin^2\theta}}{R}. \tag{2}$$

In this case, the observation window is a circle and the projection image to the observer of the observation window is also a circle, the radius of which is R_v'. The radius of actual observable space is R_v that is the minimum distance from the origin to the line ξ, which connects the observer and the boundary of the observation window. The radii R_v' and R_v are given, respectively, by

$$R_v' = R\tan(\theta - \psi), \tag{3a}$$

$$R_v = \sin\theta. \tag{3b}$$

The ratio of R_v to R_v' is given by

$$R_v / R_v' = \sin\theta / \left[R\tan(\theta - \psi)\right]. \tag{3c}$$

The radii R_v' and R_v are shown as a function of R and θ, respectively , in Figs. 3(b) and 3(c). As seen in Fig. 3(b), the radius R_v' becomes much lager than 1 when R and θ approach 1 and $90(\text{deg.})$, respectively. In this case, the actual spherical image volume is the unit sphere itself. We need to interpret the radius of actual spherical image volume, R_v, from R_v' by multiplying the ratio R_v / R_v' to R_v'. The analysis of image volume shown in Fig. 2 is to find just R_v', not R_v. In the interpretation of the numerical calculation of Section 2, we should convert R_v' distribution to R_v distribution using the ratio R_v / R_v'.

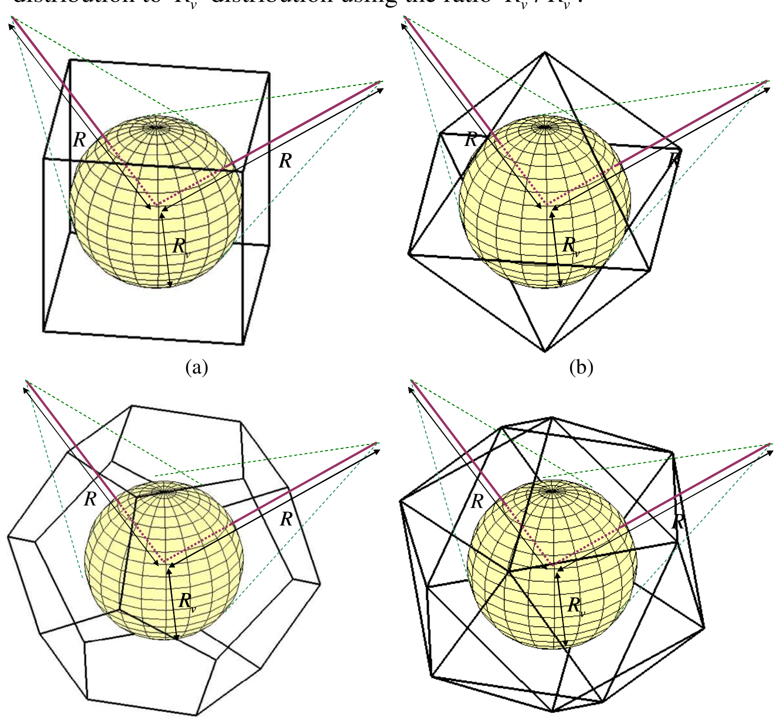

Fig. 4. Spherical image volume of regular-polyhedrons; (a) hexahedron, (b) octahedron, (c) dodecahedron, and (d) icosahedrons.

#107004 - $15.00 USD Received 30 Jan 2009; revised 24 Mar 2009; accepted 1 Apr 2009; published 2 Apr 2009

The spherical image volumes of regular-polyhedron displays are shown in Fig. 4. As indicated in Fig. 4, the observer at every observation point around regular-polyhedron displays can see the 3D object enclosed by the spherical image volume with radius of R_v.

Now, with the above stated analysis method, the main query of this paper, how the image volume size is dependent on the type of polyhedron, facet viewing angle, and observation point, is to be answered. As a result, we can figure out what type of regular polyhedron can be more favorable display structure than the others with same facet display conditions and for same observation distance. The calculation of the internal radius R_v' for many sampled points on the spherical surface with radius R_v' of Eq. (1) is repetitively performed. By multiplying Eq. (3c) to R_v', we obtain the spherical image volume radius R_v. All regular-polyhedron is inscribed polyhedron of a unit sphere with radius of 1.

In Fig. 5, the R_v distributions obtained with varying facet viewing angle θ and observation distance, R, are presented. First, we can see that there is a cut-off facet viewing angle, under which no image volume is properly defined for full 4π-solid angle parallax. Second, the dependence of image volume size on observation angle θ is more sensitive than that on the observation distance. However it should be noted that there is also a range that shows relatively steep change of the image volume size depending on the observation distance, R.

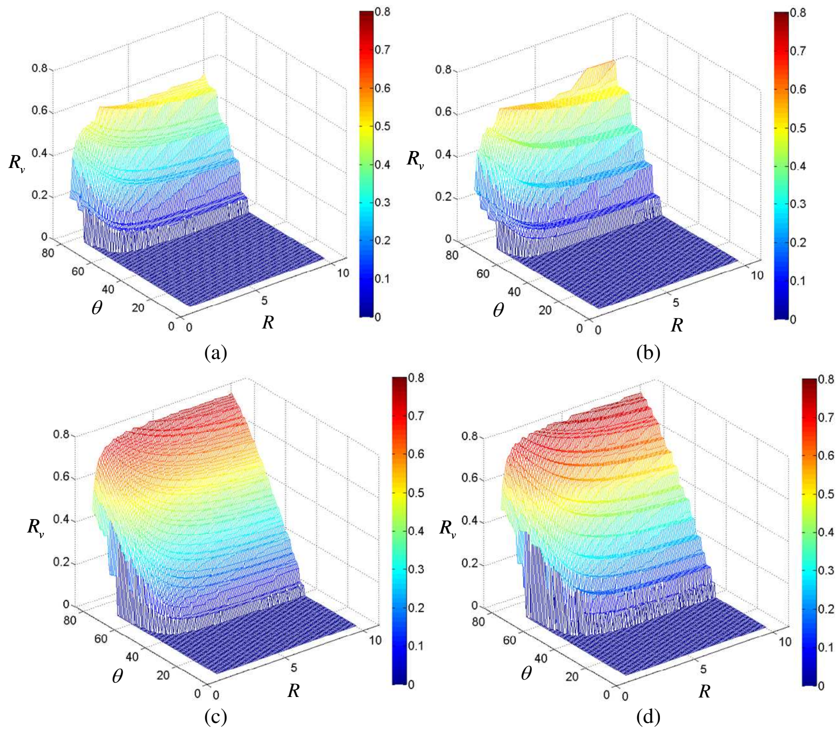

Fig. 5. Radius of spherical image volume as a function of facet viewing angle and observation distance for (a) hexahedron (viewing angle cut-off $\theta = 56$(deg.) at infinity R), (b) octahedron (viewing angle cut-off $\theta = 56$(deg.) at infinity R), (c) dodecahedron (viewing angle cut-off $\theta = 40$(deg.) at infinity R), and (d) icosahedron (viewing angle cut-off $\theta = 43$(deg.) at infinity R).

In Fig. 5(a), the image volume radius variation for facet viewing angle θ and observation distance R of hexahedron display are shown. The cut-off viewing angle for the observation distance of $R = 2$ is $\theta = 60$(deg.). At closer distance than $R = 2$, the cut-off

#107004 - $15.00 USD Received 30 Jan 2009; revised 24 Mar 2009; accepted 1 Apr 2009; published 2 Apr 2009

viewing angle becomes larger. As the observation distance R increases to infinity, the viewing angle cut-off monotonically decreases and converges to a certain value. In the case of hexahedron display, the converging viewing angle cut-off is about $\theta = 56(\text{deg.})$. Therefore, to fully use the viewing angle range of the hexahedron display, the observation distance should be lager than $R = 2$. Stepwise changes in the image volume radius for change in the facet viewing angle are perceived. In Fig. 5(b), the image volume radius variation for octahedron display is shown. At closer distance than $R = 2$, the cut-off viewing angle becomes larger than $\theta = 60(\text{deg.})$. At infinity observation distance R_∞ , the converging viewing angle cut-off is almost same value as the value of the hexahedron, $\theta = 56(\text{deg.})$. It is noteworthy that the image volume sizes of hexahedron and octahedron are almost similar even though the dihedral angle of octahedron 70.53(deg.) is much smaller than that of hexahedron 90(deg.). In the case of octahedron, the stepwise change of the image volume radius for change in facet viewing angle is more manifest than in the case of hexahedron. In Fig. 5(c), the image volume size variation for dodecahedron display is shown. In the case of dodecahedron, the converging viewing angle cut-off is about $\theta = 40(\text{deg.})$ for infinite observation distance R_∞. Figure 5(d) shows the image volume radius variation of icosahedron display. In the case of icosahedron display, the converging viewing angle cut-off is about $\theta = 43(\text{deg.})$. As a result, four regular-polyhedron displays can be classified into two kinds with respect to the image volume size property. One is the group of hexahedron and octahedron and the other is that of dodecahedron and octahedron. Among four types, dodecahedron has the lowest viewing angle cut-off, so it is a favorable structure for omnidirectional parallax 3D display.

Let us compare the image volume characteristics of regular-polyhedron displays with those of the sphere display as shown in Fig. 3. The cut-off viewing angle of the sphere display is zero (deg.) and the image volume size does not vary with the observation distance. The maximum image size of the sphere display is 1.

This analysis addresses the relationship of the image volume size to the associated structural parameters (polyhedron type, facet viewing angle, and observation radius) and provides basic design rules of the regular-polyhedron 3D display.

4. Conclusion

In conclusion, four types of conceptual 3D displays having regular polyhedron shapes, i.e., hexahedron, octahedron, dodecahedron, and icosahedron, are proposed and their structural conditions for 3D display are investigated. In principle, these regular-polyhedron 3D displays show omnidirectional parallax. However, the size of the spherical image volume containing virtual 3D objects that can be represented by those regular-polyhedron displays is finitely determined by some factors as polyhedron type, viewing angle of facet display, and observation distance. The analysis of the image volume size says that it is necessary to develop 3D flat panel with viewing angle larger than 40(deg.) for realizing omnidirectional parallax dodecahedron 3D display.

Acknowledgment

The authors acknowledge the support of the Ministry of Education, Science and Technology of Korea and the Korea Science and Engineering Foundation through the Creative Research Initiative Program (#R16-2007-030-01001-0).

#107004 - $15.00 USD Received 30 Jan 2009; revised 24 Mar 2009; accepted 1 Apr 2009; published 2 Apr 2009